Aerospace Science and Technology 105 (2020) 106051

Contents lists available at ScienceDirect

Aerospace Science and Technology

www.elsevier.com/locate/aescte

Two-layer adaptive augmentation for incremental backstepping flight control of transport aircraft in uncertain conditions

Dmitry I. Ignatyev, Hyo-Sang Shin, Antonios Tsourdos

School of Aerospace, Transport and Manufacturing, Cranfield University, Cranfield MK43 OAL, UK

ARTICLE INFO

Article history:
Received 25 July 2019
Received in revised form 5 April 2020
Accepted 24 June 2020
Available online 1 July 2020
Communicated by Efstathios Bakolas

Keywords:
Adaptive control
Parameter estimation
Incremental backstepping
Failures
Fault-tolerant control

ABSTRACT

Presence of uncertainties caused by unforeseen malfunctions in actuation system or changes in aircraft behaviour could lead to aircraft loss-of-control during flight. The paper presents Two-Layer Adaptive augmentation for Incremental Backstepping (TLA-IBKS) control algorithm designed for a large transport aircraft. IBKS uses angular accelerations and current control deflections to reduce the dependency on the aircraft model. However, it requires knowledge of control effectiveness. The proposed technique is capable to detect possible failures for an overactuated system. At the first layer, the system performs monitoring of a combined effectiveness and detects possible failures via an innovation process. If a problem is detected the algorithm initiates the second-layer algorithm for adaptation of effectiveness of individual control effectors. Filippov generalization for nonlinear differential equations with discontinuous right-hand sides is utilized to develop Lyapunov based tuning function adaptive law for the second layer adaptation and to prove uniform asymptotic stability of the resultant closed-loop system. Conducted simulation manifests that if the input-affine property of the IBKS is violated, e.g., in severe conditions with a combination of multiple failures, the IBKS can lose stability. Meanwhile, the proposed TLA-IBKS algorithm demonstrates improved stability and tracking performance.

1. Introduction

Enabling flight safety of passenger aviation in the presence of abnormal conditions, such as those caused by equipment failures and/or adverse environmental factors, is a vital problem. Analysis of accident and incidence reports revealed that the main contribution to the fatal accidents were due to aircraft Loss of Control In-Flight and Controlled Flight Into Terrain [1]. The main reasons caused these accidents are pilot mistakes, technical malfunctions, or their combination.

Recently, great efforts have been undertaken to develop aircraft control design tools and techniques for enabling safe flight [2–8]. The idea that non-conventional control strategies can prevent possible accidents and recover aircraft from dangerous situations stimulates researches toward fault-tolerant and adaptive flight control [9–12].

Gain-scheduling of linear feedback controllers is widely applied in commercial applications to achieve stabilization and satisfactory tracking performance of aircraft over a wide range of flight conditions [13], [14]. In case of severe and unpredicted changing in aircraft behaviour such controllers cannot be used or can be used only with a restricted functionality.

Nonlinear Dynamics Inversion (NDI) and Backstepping (BS) techniques have become popular control strategies for adaptation since they can be used for global linearization of the system dynamics and control decoupling [15–19]. The BS control has advantages in comparison with the NDI, namely, it is more flexible and it is based on Lyapunov stability theory. Later, to make the NDI and BS controls more robust and fault-tolerant an incremental-type sensor-based form has been proposed [20–22].

However, even in this formulation the controller still requires accurate knowledge of the control effectiveness, especially, if the system is not affine in control inputs because of non-linearity in actuators or due to large transport delays. Additional adaptation strategies augmenting the incremental-type controllers to reduce dependency on an aircraft model were applied for a high-performance aircraft model in [23], [24]. Adaptive strategy helped to improve performance of IBKS control of the hypersonic interceptor [25]. Regardless of the fact that IBKS demonstrates robustness to some failures [26] estimation of the control effectiveness improves fault-tolerant abilities of the system [27], [28].

It is well known that one of the main challenges of an online estimation is that it is carried out while a control system is oper-

E-mail address: d.ignatyev@cranfield.ac.uk (D.I. Ignatyev).

https://doi.org/10.1016/j.ast.2020.106051

ating [29]. It is common for an automatic control system to move several control surfaces in a proportional manner, bringing about nearly exact linear correlation between control surfaces. In addition, modern passenger aircrafts have many control effectors for both longitudinal and lateral control, so the multiple-input problem appears. Dedicated manoeuvres that maximise the observability of the parameters to be estimated, for example, individual rudder or aileron steps, cannot be carried out. Thus, the identification capabilities of the algorithm are limited, especially, in case of failures.

Reliable identification can be achieved via the maximization of the information content in the data using proper excitations of the system. On the other hand, excessive system excitation because of ongoing manoeuvres can cause several undesired consequences, such as a decrease in passenger comfort during flight or decrease of control performance. But, estimation algorithms without persistent excitation could suffer from estimator windup [30], which is unbounded growth of adaptation gains, making the estimator algorithm sensitive to noise. Thus, the identification routine should be a trade-off between identification precision and performance requirements. Such constraints leave an imprint on the online identification routine.

The present paper demonstrates results from the European project INCEPTION, which is seeking the development of fault-tolerant Automatic Flight Control System for fixed-wing aircraft allying incremental control strategies, adaptive augmentation and envelope protection [31]. Two-Layer Adaptive augmentation to IBKS control law (TLA-IBKS) is developed in the current study. The proposed augmentation is designed to improve stability and tracking performance of the IBKS baseline controller by providing actual information about control effectiveness in case of uncertainty or failure.

The first layer is responsible for detecting anomalies in the control effectiveness of the overactuated system, while the second layer is designed to determine and update the effectiveness of the individual effector detected as failed. At the first layer, the system performs monitoring of the combined effectiveness and detects possible failures via the generation of an innovation process. The innovation process is defined as the difference between the actual system output and the expected output based on the model and the previous output data. The first layer governs the control effectiveness estimation in the second layer. If a problem in the combined control effectiveness is detected, the algorithm activates the second-layer estimation of the individual effectiveness and stops the adaptation algorithm at the second layer when the difference between the actual system output and the updated model output becomes small. Such a structure helps to design a fault-tolerant control without making assumptions about a fault type. Activation and termination of the second layer adaptation by the first layer cause discontinuity of the closed-loop system dynamics and thus classical Lyapunov based approach is not applicable to design an adaptive control law. Filippov generalization for nonlinear differential equations with discontinuous right-hand sides is adopted to develop Lyapunov based TF adaptive law for the second layer adaptation and to prove uniform asymptotic stability of the resultant closed-loop system. Simulation results demonstrate the effectiveness of the proposed structure in tackling the model uncertainties.

The paper is organized in the following way. A very brief overview of the flight dynamics and IBKS control strategy are given in Sections 2 and 3 correspondingly. Section 4 provides a description of the two-layer identification framework in general. The first layer algorithm is considered in Sections 5. The development of the second layer adaptation law and proof of the closed-loop system stability with the proposed two-layer structure is discussed in Section 6. Section 7 deals with a simulation study of the proposed framework. In particular, proposed TF adaptive algorithm is compared with the Recursive Least Squares bases adaptation. Finally, concluding remarks are articulated in Section 8.

2. Flight dynamics model

Equations of motions of the aircraft can be represented with kinematics and dynamics models. The kinematics of the aircraft is described by the attitude state vector $\boldsymbol{\xi} = [\phi\ \theta\ \beta]^T$, where ϕ, θ, β are roll, pitch and sideslip angles.

$$\dot{\boldsymbol{\xi}} = \mathbf{f}_\xi + T_\xi \boldsymbol{\omega} \tag{1}$$

where

$$\mathbf{f}_\xi = \begin{bmatrix} 0 & 0 & -\dfrac{A_x}{V_t}\cos\alpha\sin\beta + \dfrac{A_y}{V_t}\cos\beta - \dfrac{A_z}{V_t}\sin\alpha\sin\beta + \dfrac{g_y}{V_t} \end{bmatrix}^T,$$

$$T_\xi = \begin{bmatrix} 1 & \sin\phi\tan\theta & \cos\phi\tan\theta \\ 0 & \cos\phi & -\sin\phi \\ \sin\alpha & 0 & -\cos\alpha \end{bmatrix},$$

$\boldsymbol{\omega} = [p, q, r]^T$ is the rotational rate vector. Specific forces A_x, A_y and A_z can be directly measured by the accelerometers. V_t is the true airspeed, α is the angle of attack, g_y is the y-axis component of the gravitational acceleration calculated in the wind reference frame.

The aircraft dynamics is represented with the state-space form for the state vector $\mathbf{y} = [V_t\ p\ q\ r]^T$ composed of airspeed V_t, roll rate p, pitch rate q and yaw rate r.

$$\dot{\mathbf{y}} = \mathbf{f}_y(\mathbf{y}, \mathbf{u}) \tag{2}$$

Control inputs $\mathbf{u} = [\delta_{ail_{IL}} \delta_{ail_{IR}} \delta_{ail_{OL}} \delta_{ail_{OR}} \delta_{e_{IL}} \delta_{e_{IR}} \delta_{e_{OL}} \delta_{e_{OR}} \delta_{r_u} \delta_{r_l} \delta_{T_{IL}} \delta_{T_{IR}} \delta_{T_{OL}} \delta_{T_{OR}}]^T$ are the inner-left, inner-right, outer-left, and outer-right ailerons; inner-left, inner-right, outer-left, and outer-right elevators; upper and lower rudders; outer-left, inner-left, inner-right, and outer-right engines throttle.

The nonlinear dynamics $\mathbf{f}_y(\mathbf{y}, \mathbf{u})$ is linearized using the incremental dynamics approach for the incremental controller design and thus the precise description is not provided here.

3. Incremental backstepping

Sensor-based technique utilizing Incremental Dynamics (ID) applied to obtain an IBKS controller, which is less dependent on the system model, is discussed in [32], [33]. Below, we will just provide a brief description of this controller. Details could be found in the original papers. IBKS computes incremental commands employing acceleration feedback estimations to extract unmodelled dynamics information. In the present study, we are using this controller as a baseline controller, which is augmented with the two-layer online parameter estimation framework.

3.1. Incremental dynamics model

Let us assume that a system dynamics is described by the following equation:

$$\dot{\mathbf{x}} = \mathbf{f}_\mathbf{x}(\mathbf{x}, \mathbf{u}) \tag{3}$$

where $\mathbf{f}_\mathbf{x} : \mathbb{R}^n \times [0, \infty) \to \mathbb{R}^n$ is Lipschitz continuous function, $\mathbf{x}$ and $\mathbf{u}$ are the state and the control input vectors. Expanding (3) into the Taylor series around $(\mathbf{x}_0, \mathbf{u}_0)$ corresponding to the previous time moment t_0 the dynamics (3) can be expressed in the following form

$$\dot{\mathbf{x}} \cong \dot{\mathbf{x}}_0 + \frac{\partial \mathbf{f}_\mathbf{x}(\mathbf{x}, \mathbf{u})}{\partial \mathbf{x}}(\mathbf{x} - \mathbf{x}_0) + \frac{\partial \mathbf{f}_\mathbf{x}(\mathbf{x}, \mathbf{u})}{\partial \mathbf{u}}(\mathbf{u} - \mathbf{u}_0) \tag{4}$$

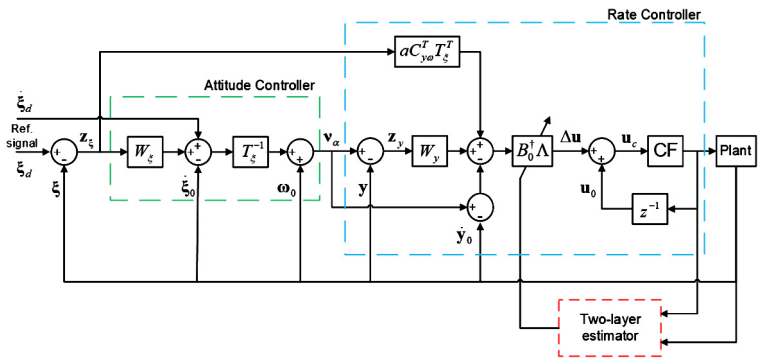

Fig. 1. Controller structure.

Assuming that the increment in state $\Delta\mathbf{x} = \mathbf{x} - \mathbf{x}_0$ is much smaller than the increment in both state derivative $\Delta\dot{\mathbf{x}} = \dot{\mathbf{x}} - \dot{\mathbf{x}}_0$ and input $\Delta\mathbf{u} = \mathbf{u} - \mathbf{u}_0$, the dynamics (4) can be simplified

$$\Delta\dot{\mathbf{x}} \cong B_0 \Delta\mathbf{u} \tag{5}$$

where $B_0 = \frac{\partial \mathbf{f}_{\mathbf{x}}(\mathbf{x},\mathbf{u})}{\partial \mathbf{u}}$ is a control effectiveness matrix.

The dynamics equation in the form (5) articulates that ID of the system is produced by the control input increment. For implementation of such a concept it is assumed that sampling time is small. In this case, the assumption that $\Delta\mathbf{x} \ll \Delta\dot{\mathbf{x}}$ and $\Delta\mathbf{x} \ll \Delta\mathbf{u}$ becomes possible for the real aircraft because the control surface deflections directly effect the angular accelerations, whereas the angular rates are only changed by integrating these angular accelerations. Actuators are assumed to be instantaneously fast such that the demanded input increment can be achieved within the small sampling time. In addition, the sensors are assumed to be ideal, i.e. providing state derivative without errors.

3.2. Attitude controller

The ID idea combined with the backstepping paradigm was used to design the aircraft baseline controller. To increase the control robustness and simplify its implementation, both angle and rate controllers using ID were formulated. The general structure of the baseline controller, manifesting the interaction between attitude and rate controllers, is provided in Fig. 1.

Equations (1) and (2) constitute the system dynamics. Introducing the kinematics tracking error variable $\mathbf{z}_\xi = \boldsymbol{\xi}_d - \boldsymbol{\xi}$, where $\boldsymbol{\xi}_d$ is the desired kinematics state vector, the sub-system (1) can be reformulated in terms of $\mathbf{z}_\xi$:

$$\dot{\mathbf{z}}_\xi = \dot{\boldsymbol{\xi}}_d - \mathbf{f}_\xi - T_\xi \boldsymbol{\omega} \tag{6}$$

The general idea behind the backstepping is to consider the state vector $\boldsymbol{\omega} = [p\ q\ r]^T$ from (2) as a control input for $\mathbf{z}_\xi$ subsystem (6). Since $\boldsymbol{\omega}$ is just a state variable and not the real control input, it is called a virtual control input.

For the $\mathbf{z}_\xi$ subsystem a Candidate Lyapunov Function (CLF) V_ξ is selected:

$$V_\xi = \frac{1}{2}\mathbf{z}_\xi^T \mathbf{z}_\xi, \tag{7}$$

which is positive for the whole domain, excluding the origin, where it equals to zero.

For the asymptotic convergence of the error, the CLF derivative must be strictly negative along the solutions of (6). Considering a positive definite matrix $W_\xi \in \mathbb{R}^{3\times3}$, the CLF is strictly negative if:

$$\dot{V}_\xi = \mathbf{z}_\xi^T \dot{\mathbf{z}}_\xi = -\mathbf{z}_\xi^T W_\xi \mathbf{z}_\xi. \tag{8}$$

The kinematics tracking error dynamics can be represented in the incremental form

$$\dot{\mathbf{z}}_\xi = \dot{\boldsymbol{\xi}}_d - \dot{\boldsymbol{\xi}}_0 - T_\xi (\boldsymbol{\omega} - \boldsymbol{\omega}_0). \tag{9}$$

Substituting the expression $\dot{\mathbf{z}}_\xi = -W_\xi \mathbf{z}_\xi$ derived from (8), the following tracking error dynamics is obtained

$$\dot{\boldsymbol{\xi}}_d - \dot{\boldsymbol{\xi}}_0 - T_\xi (\boldsymbol{\omega} - \boldsymbol{\omega}_0) + W_\xi \mathbf{z}_\xi = 0. \tag{10}$$

The virtual control law $\boldsymbol{\nu}_\alpha = \boldsymbol{\omega}$ can be obtained by inversion of (10) with respect to $\boldsymbol{\omega}$

$$\boldsymbol{\nu}_\alpha = \boldsymbol{\omega}_0 + T_\xi^{-1}\left(W_\xi \mathbf{z}_\xi + \dot{\boldsymbol{\xi}}_d - \dot{\boldsymbol{\xi}}_0\right), \tag{11}$$

since T_ξ is invertible for the transport aircraft within the flight envelope. The control law (11) is used as a desired value for the virtual control input $\boldsymbol{\omega}$.

3.3. Rate controller

The difference between the dynamics state variable $\mathbf{y} = \left[V_t \boldsymbol{\omega}^T\right]^T$ and its desired value $\mathbf{y}_d = \left[V_{td} \boldsymbol{\omega}_d^T\right]^T$ is defined as the dynamics tracking error variable $\mathbf{z}_y = \mathbf{y}_d - \mathbf{y}$. It should be noted that the airspeed is introduced as a state to the dynamics state vector in order to design the controller that simultaneously tracks the airspeed and angular rates of the aircraft. To design a control law $\mathbf{u}$ that ensures that $\mathbf{z}_y$ converges to zero, the following CLF for the complete $(\mathbf{z}_\xi, \mathbf{z}_y)$-system is formed:

$$V_y = V_\xi + \frac{1}{2a}\mathbf{z}_y^T \mathbf{z}_y, \tag{12}$$

where a is a design scale factor. Similar to design of CLF for the $\mathbf{z}_\xi$ subsystem in (8), here a matrix $W_y \in \mathbb{R}^{4\times4}$ is assumed to be a positive definite matrix such that

$$\dot{V}_y = \dot{V}_\xi + \frac{1}{a}\mathbf{z}_y^T \dot{\mathbf{z}}_y = -\mathbf{z}_\xi^T W_\xi \mathbf{z}_\xi - \frac{1}{a}\mathbf{z}_y^T W_y \mathbf{z}_y. \tag{13}$$

Thus, the error $\mathbf{z}_y$ converges asymptotically to zero since the derivative of the CLF V_y is strictly negative for non-zero errors. The following tracking error dynamics in the incremental representation has the following form:

$$\dot{\mathbf{z}}_y = \dot{\mathbf{y}}_d - \dot{\mathbf{y}}_0 - B_0 (\mathbf{u} - \mathbf{u}_0), \tag{14}$$

where $B_0 = \frac{\partial \mathbf{f}_{\mathbf{x}}(\mathbf{x},\mathbf{u})}{\partial \mathbf{u}}$ is the control effectiveness matrix.

The selection matrix $C_{y\omega} = \begin{bmatrix} \mathbf{0}_3 & I_3 \end{bmatrix}$, which performs the mapping $\boldsymbol{\omega} = C_{y\omega}\mathbf{y}$, is introduced. Combining the incremental dynamics of $\mathbf{z}_\xi$ (10) and $\mathbf{z}_y$, one can obtain

$$\mathbf{z}_{\xi}^{T}\left(\dot{\boldsymbol{\xi}}_{d}-\dot{\boldsymbol{\xi}}_{0}-T_{\xi}\left(\boldsymbol{\nu}_{\alpha}-C_{y\omega}\mathbf{z}_{y}-\boldsymbol{\omega}_{0}\right)+W_{\xi}\mathbf{z}_{\xi}\right)+\frac{1}{a}\mathbf{z}_{y}^{T}\left(\dot{\mathbf{y}}_{d}-\dot{\mathbf{y}}_{0}-B_{0}\left(\mathbf{u}-\mathbf{u}_{0}\right)+W_{y}\mathbf{z}_{y}\right). \tag{15}$$

Eventually, for non-zero errors, substituting (11) into (15) and solving it with respect to $\mathbf{u}$, the resultant control law is designed

$$\mathbf{u}_{c}=\mathbf{u}_{0}+B_{0}^{-1}\Lambda\left(aC_{y\omega}^{T}T_{\xi}^{T}\mathbf{z}_{\xi}+W_{y}(\mathbf{y}_{d}-\mathbf{y})+\dot{\mathbf{y}}_{d}-\dot{\mathbf{y}}_{0}\right) \tag{16}$$

To attenuate the measurement noise and increase the control robustness, B_0 is multiplied by a diagonal matrix $\Lambda > 0$ with elements $\lambda_{ii} \in [0, 1]$.

The control law in the form (16) requires inversion of the matrix B_0, which is not square for the overactuated modern transport aircraft. To tackle this issue, Moore-Penrose Pseudo-inverse is applied [33], and

$$B_{0}^{\dagger}=B_{0}^{T}\left(B_{0}B_{0}^{T}\right)^{-1} \tag{17}$$

is used in (16) instead of B_0.

3.4. Command filter

To avoid infeasible commands provided by the controller, a Command Filter (CF) is added to the controller output. For incremental controllers, the CF is used to constrain the input to respect the actuators dynamics and saturation.

Taking into account the influence of the CF $\boldsymbol{\chi} \in \mathbb{R}^3$ on the tracking error $\mathbf{z}_y$ (14) the dynamics of the modified tracking error $\bar{\mathbf{z}}_y$ is introduced [23]

$$\dot{\bar{\mathbf{z}}}_{y}=\dot{\mathbf{y}}_{d}-\dot{\mathbf{y}}_{0}-B_{0}\left(\mathbf{u}-\mathbf{u}_{0}\right)-\dot{\boldsymbol{\chi}} \tag{18}$$

Effect of the CF on the tracking error can be estimated by the stable linear filter [23]:

$$\dot{\boldsymbol{\chi}}=-W_{y}\boldsymbol{\chi}+B_{0}\left(\mathbf{u}_{CF}-\mathbf{u}_{c}\right), \tag{19}$$

where $\mathbf{u}_{CF}$ is the controller output after CF.

4. Two-layer estimator

Finally, the cascaded baseline controller consists of attitude and rate controllers (11) and (16). Both attitude and rate controllers have the similar control structure, namely, the control signal compensating the difference between the reference and measured (or estimated) state variables is added to the current value of the control value. Such a structure is very simple and robust to the model uncertainties. However, to ensure stability and performance of the algorithm, the precise knowledge of the control input matrices T_ξ and B_0 is required. The precise value of T_ξ within the flight envelope can be easily determined because it represents the kinematic relationships. The matrix B_0 specifies the control effectiveness, which might change during flight because of changing of environmental conditions, structural deformations, failures etc. Hence, an unmodelled actuator dynamics is a source of uncertainty.

The main purpose of the adaptive augmentation for the IBKS is to compensate the effect of these uncertainties and to improve performance and stability of the IBKS controller. This paper introduces a two-layer identification framework detecting, isolating anomalies and estimating the aircraft control derivatives B_0 when uncertainties are in the actuation system. Interaction of the adaptive augmentation with the baseline controller is demonstrated in Fig. 1. The adaptive block performs fault detection, isolation, estimation and adaptation of the control effectiveness matrix B_0.

The two-layer estimator structure is designed to avoid excessive system excitation. The high-level structure of the interaction between the proposed framework with the baseline controller and the aircraft is shown in Fig. 2. The first layer is a supervising algorithm that activates second layer identification if any discrepancy between the on-board model and the estimated generalized parameter is observed. At the second level, the values of individual control effectiveness are estimated. The identification manoeuvres are demanded together with the second layer activation. At the same time, if a new estimated value suits the model, the first layer turns off the estimation process of the second layer. In addition to reducing the required system excitation, such a strategy makes possible parameter estimations under limited system excitations.

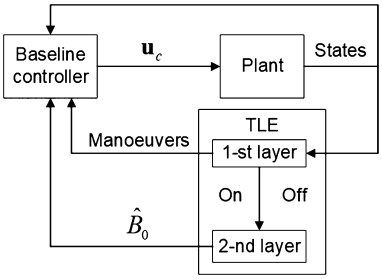

Fig. 2. High-level representation of the system.

5. First layer

Reliability of the identification results could be achieved via maximization of the information content in the data using proper excitations of the system. On the other hand, excessive system excitation could cause several undesired consequences, such as a decrease in passenger comfort during flight or decrease of a mission accomplishment performance because of ongoing manoeuvres. Thus designed identification routine should be a trade-off between identification precision and mission performance requirements.

An aircraft flight control system sends the same signals for all individual control surfaces, making the individual signals are proportional to each other and causing a high-correlation between the individual signals. If all the input signal forms look the same, then any algorithm trying to assign values for the control effectiveness of each individual control will fail, because it is impossible to determine which of the multiple inputs, moved in the same manner, was responsible for changes in the aerodynamic forces and moments. Input forms that are completely decorrelated will give the most accurate control effectiveness estimates. Unfortunately, when a feedback control system is operating, desired input forms become distorted by the feedback control.

Since the main uncertainty of the proposed control law is considered to be in the control effectiveness, a combined effectiveness, which essentially treats all of the correlated control surfaces as if they were a single control surface [29], is used as a generalized system parameter. The combined effectiveness was used in fault detection and isolation in [28], [34].

5.1. Combined effectiveness estimation

The combined effectiveness for each of the component of the dynamic state $\mathbf{y} = [V\ p\ q\ r]$ is estimated from the regression model independently

$$\boldsymbol{\varsigma}_{m} \cong \mathbf{A}\hat{\theta}_{m}, \tag{20}$$

where $\boldsymbol{\varsigma}_m = [\Delta\dot{y}_m(1)\,\Delta\dot{y}_m(2)\ldots\Delta\dot{y}_m(N)]$ is the response variable vector, $\Delta\dot{y}_m(1)\,\Delta\dot{y}_m(2)\ldots\Delta\dot{y}_m(N)$ is the record of derivative increment for m component of the dynamic state vector $\mathbf{y}$, $\mathbf{A} = [\Delta u_c(1)\,\Delta u_c(2)\ldots\Delta u_c(N)]$ is a predictor variable,

$\Delta u_c(1)\,\Delta u_c(2)\ldots\Delta u_c(N)$ is the record of increment of the combined control effector in m direction, $\hat{\theta}_m$ is the combined control effectiveness, which is a parameter to be identified.

The combined control effector in m direction is calculated using the following equation:

$$\Delta u_c(t) = \sum_{i=1}^{N_u} \hat{b}_{m_i} \Delta u_i(t) \Big/ \sum_{i=1}^{N_u} \hat{b}_{m_i}, \tag{21}$$

where $\hat{b}_{m_i}$ is the estimation of individual effectiveness of control effector i in m direction obtained in the previous periods, u_i is the control input form effector i at time moment t, N_u is a number of effectors. It is assumed that at least one effector is available for each of the control direction m.

The combined effectiveness serves as a generalized parameter that is used for monitoring of the system state. Monitoring only one parameter reduces the computation costs of the algorithm as compared to monitoring the state of each effector.

5.2. Recursive least square with modified exponential forgetting

The combined effectiveness is estimated online using the Recursive Least Square (RLS) with exponential forgetting (EF), which is commonly used for the real-time system identification. The technique enables recursive computations of estimates to be carried out. The typical algorithm for EF RLS is

$$\begin{aligned} &\hat{\boldsymbol{\theta}}(t) = \hat{\boldsymbol{\theta}}(t-1) + P(t)\boldsymbol{\varphi}(t)\left[y(t) - \boldsymbol{\varphi}^T(t)\hat{\boldsymbol{\theta}}(t-1)\right], \\ &R(t) = F(t)R(t-1) + \boldsymbol{\varphi}(t)\boldsymbol{\varphi}^T(t), \\ &F = \mu I \end{aligned} \tag{22}$$

where $\hat{\boldsymbol{\theta}}(t) \in R^n$ is the estimates of the parameter vector at time step t, $\boldsymbol{\varphi}(t) \in R^n$ is the observer data vector, $y(t) \in R$ is the system output vector, $P(t) \in R^{n\times n}$ is the covariance matrix, $R(t) \in R^{n\times n}$ is the information matrix that is inverse of the covariance matrix, $F(t) \in R^{n\times n}$ is the forgetting matrix, $\mu \in (0, 1)$ is the scalar forgetting factor.

It is well known that EF RLS shows good results under the persistent excitation (PE) conditions. However, this condition is hardly possible in the real flight conditions of transport aircraft, for example, during the cruise flight. If the PE is not achieved the EF RLS could suffer from estimator windup [30]. To tackle this problem the following modification of EF algorithm was proposed in [35]

$$F(t) = \mu I + \delta P(t-1), \tag{23}$$

where $\delta > 0$ is a design parameter. This modification guarantees the boundedness of the information matrix, while maintaining the convergence characteristics of the EF algorithm. It was shown in [35] that, where the PE condition does not hold, the following information matrix evaluation is true

$$R(t) \geq \frac{\delta}{1-\mu} I \quad \forall t.$$

Therefore, the covariance matrix is uniformly bounded from above even without PE in the proposed algorithm. The lower bound of the information matrix is determined by δ, μ, and excitation of $\boldsymbol{\varphi}(t)\boldsymbol{\varphi}^T(t)$. This implies that the lower bound can be controlled within the proposed algorithm.

5.3. Failure detection

Generally, a fault of the actuation system cause a change in aerodynamic effectiveness, which is captured by combined effectiveness estimations $\hat{\theta}_m$ through (20)–(23). To detect possible failures, the current state of aerodynamic efficiency is evaluated in comparison with the model one. The model combined effectiveness is based on the information received in the previous periods and computed through the following equation

$$\bar{\theta}_m(t) = \sum_{i=1}^{N_u} \hat{b}_{m_i} \Delta u_i(t) \Big/ \sum_{i=1}^{N_u} \Delta u_i(t). \tag{24}$$

The error signal of the observation i is calculated as the difference between the estimated combined effectiveness and the expected effectiveness based on the model and the previous data:

$$e_i = \hat{\theta}_{m_i} - \bar{\theta}_m. \tag{25}$$

Under normal conditions, the error signal is “small” and corresponds to random fluctuations in the output since all the systematic trends are predicted by the model. However, under faulty conditions, the error signal is significant and contains systematic trends because the model no longer represents the physical system adequately.

Among different fault types that can arise in the system, in the current study, we consider only actuator faults that can be described with first and second-order actuator dynamics, which can be used for wide class of failures [36], [37]. These faults make the error signal depart from the zero mean. Hence, it is useful to perform the statistical test of the zero mean. The mean of the error signal sequence is estimated as

$$\bar{e} = \frac{1}{n}\sum_{i=1}^{n} e_i,$$

where n is the sample-size. The standard deviation is estimated as follows

$$\sigma_{st} = \frac{1}{n-1}\sum_{i=1}^{n} e_i^2.$$

We introduce T-statistics calculated for the mean of the error signal as a measurable criterion for decision making [38]:

$$T_{stat} = (\bar{e} - \mu) \Big/ \left((\sigma_{st} + b)/\sqrt{n}\right) \tag{26}$$

where μ is the population mean. Since the test checks whether the sequence has zero mean, $\mu = 0$. The bias b is introduced to increase the tolerance of the detection procedure to “small” errors of the identification algorithm.

The calculated statistics is tested against two hypotheses:

$$H_0 : T_{stat} < T_{\alpha/2}, H_1 : T_{stat} \geq T_{\alpha/2} \tag{27}$$

The following interpretation can be obtained as a result of testing (27):

(1) Rejecting H_0 (accepting H_1): there is significant evidence that the error is not zero and the error can be due to a fault.
(2) Keeping H_0: we do not have enough evidence to believe that there is a fault.

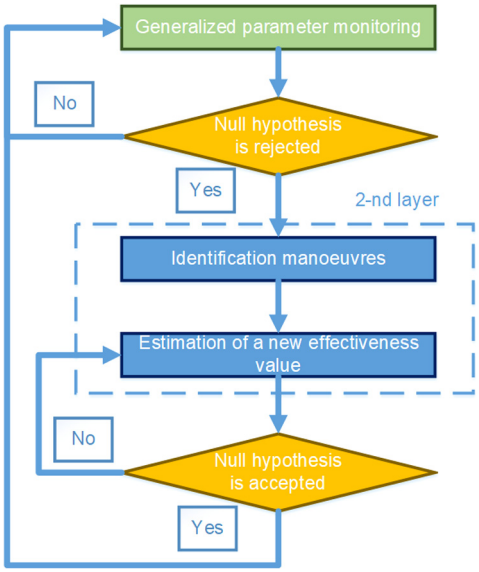

Fig. 3. Operational diagram of the online identification routine.

6. Second layer of identification

If the system detects any deviation from the nominal operational regime in one of the control direction, the system steps into the second layer of estimator where the failure is localized and the individual effectiveness is evaluated (see Fig. 3).

As it was mentioned before, identification of individual control effectiveness is complicated with a high-correlation between the individual signals. To tackle this issue, we use a priori information through fixing the effectiveness of all but one of the correlated control surfaces to a priori values [29].

While identifying the effectiveness of a certain control surface, the aircraft is demanded to perform manoeuvres with reduced coefficients in the allocation matrix $W_s D_u$ for all control effectors responsible for the motion, except the coefficient relating to the elevator under study. In such a case, the control signal is split into two signals, the first one is for the control surface of which effectiveness is treated, while the second signal is for all other surfaces from the pool. Thus, the first signal is responsible for generating the required information for identification and second one is used for guaranteeing the aircraft stability.

In the current section, we would like to design an adaptive augmentation to the baseline IBKS controller using the Tuning Function (TF) approach [17]. Meanwhile, in the proposed concept the second-layer adaptation is supervised by the first layer algorithm monitoring T-statistics (27) and thus the adaptation becomes a non-smooth and time-dependent process. To prove stability of the system in case of two-layer adaptation let us consider the system in the general form.

Existence and uniqueness of the continuous solution $\mathbf{x}$ of (3) are provided under the condition that the function $\mathbf{f_x}$ is Lipschitz continuous. However, in the current study, we consider that the second layer adaptation is activated by the external process - the first-layer estimator - as a result of failure detection and, in the general case, makes $\mathbf{f_x}$ discontinuous.

If $\mathbf{f_x}$ contains a discontinuity, then a solution to (3) may not exist in the classical sense. Utilizing differential inclusions, the value of a generalized solution (e.g., [39] Filippov solution) at a certain point can be found by interpreting the behaviour of its derivative at nearby points. Generalized solutions will be close to the trajectories of the actual system since they are a limit of solutions of ordinary differential equations with a continuous right-hand side.

Before design of the estimation law, let us introduce the following important definitions.

6.1. Preliminaries

Definition 1 *(Filippov solution).* A function $\mathbf{x}$ is called a solution of (3) on the interval $[t_0, t_1]$ if it is absolutely continuous on $[t_0, t_1]$ and for almost all $t \in [t_0, t_1]$

$$\dot{\mathbf{x}} \in \mathbf{K}[\mathbf{f}](\mathbf{x}, t) \tag{28}$$

where

$$\mathbf{K}[\mathbf{f}](\mathbf{x}, t) \triangleq \bigcap_{\delta>0} \bigcap_{\mu N=0} \bar{co}\, \mathbf{f}(B(\mathbf{x}, \delta) \setminus N, t) \tag{29}$$

$\bigcap_{\mu N=0}$ denotes the intersection over all sets N of Lebesgue measure zero, $\bar{co}$ denotes convex closure and $B(\mathbf{x}, \delta) = \left\{ \mathbf{v} \in \mathbb{R}^n \middle| \|\mathbf{x} - \mathbf{v}\| < \delta \right\}$.

Definition 2. The generalized directional derivative is introduced [40]:

$$\mathbf{f}^{\circ}(\mathbf{x}, \mathbf{v}) = \lim_{\mathbf{y} \to \mathbf{x}} \sup_{t \to +0} \frac{\mathbf{f}(\mathbf{y} + t\mathbf{v}) - \mathbf{f}(\mathbf{y})}{t} \tag{30}$$

Definition 3 *(Regular function).* [40]. Function $\mathbf{f}(\mathbf{x}) : \mathbb{R}^m \to \mathbb{R}^n$ is called to be regular at $\mathbf{x} \in \mathbb{R}^m$ if for all $\mathbf{v} \in \mathbb{R}^m$, the right directional derivative of $\mathbf{f}$ at $\mathbf{x}$ in the direction of $\mathbf{v}$ exists and $\mathbf{f}'(\mathbf{x}, \mathbf{v}) = \mathbf{f}^{\circ}(\mathbf{x}, \mathbf{v})$.

Theorem 1 *(Chain rule). [41]. Let $\mathbf{x}$ be a Filippov solution of (3) on an interval containing t and $V : \mathbb{R}^n \times [0, \infty) \to \mathbb{R}$ be a locally Lipschitz, regular function. Then $V(\mathbf{x}(t), t)$ is absolutely continuous, $\frac{d}{dt} V(\mathbf{x}(t), t)$ exists almost everywhere (a.e.) and*

$$\frac{d}{dt} V(\mathbf{x}(t), t) \overset{a.e.}{\in} \dot{\tilde{V}}(\mathbf{x}, t) \tag{31}$$

where

$$\dot{\tilde{V}}(\mathbf{x}, t) \triangleq \bigcap_{\xi \in \partial V(\mathbf{x}, t)} \xi^T \begin{pmatrix} \mathbf{K}[\mathbf{f}](\mathbf{x}, t) \\ 1 \end{pmatrix} \tag{32}$$

The stability theorems are stated in terms of the set valued map $\dot{\tilde{V}}$ [41].

Theorem 2 *(Stability). Let $\mathbf{f}(\mathbf{x}, t)$ be essentially locally bounded and $0 \in \mathbf{K}[\mathbf{f}](0, t)$ in a region $Q \supset \{\mathbf{x} \in \mathbb{R}^n \,|\, \|\mathbf{x}\| < r\} \times \{t \,|\, t_0 \le t < \infty\}$. Also, let $V : R^n \times R \to R$ be a regular function satisfying*

$$V(0, t) = 0 \tag{33}$$

and

$$0 < V_1(\|\mathbf{x}\|) \le V(\mathbf{x}, t) \le V_2(\|\mathbf{x}\|) \text{ for } \mathbf{x} \ne 0 \tag{34}$$

in Q for some class K (a definition of class K functions can be found in [42]). Then,

1. *$\dot{\tilde{V}}(\mathbf{x}, t) \le 0$ in Q implies $\mathbf{x}(t) \equiv 0$ is a uniformly stable solution.*
2. *If in addition, there exists a class K functions ϖ in Q with the property*

$$\dot{\tilde{V}}(\mathbf{x}, t) \le -\varpi(\mathbf{x}) < 0 \tag{35}$$

then the solution $\mathbf{x}(t) \equiv 0$ is uniformly asymptotically stable.

6.2. Estimation law

Here, we assume that actuator failure causes degradation of the actuation effectiveness. The dynamics of the general tracking error dynamics $\mathbf{z}_g = \begin{bmatrix} \mathbf{z}_\xi^T & \mathbf{z}_y^T \end{bmatrix}^T \in R^7$, which is measurable system state, is introduced with the following equations

$$\begin{aligned} \dot{\mathbf{z}}_\xi &= \dot{\boldsymbol{\xi}}_d(t) - \dot{\boldsymbol{\xi}}_0(\mathbf{z}_g, t) - T_\xi\left(\boldsymbol{\omega}(\mathbf{z}_g, t) - \boldsymbol{\omega}_0(\mathbf{z}_g, t)\right), \\ \dot{\bar{\mathbf{z}}}_y &= \dot{\mathbf{y}}_d(\boldsymbol{\omega}_0, t) - \dot{\mathbf{y}}(\mathbf{z}_g, t) - B_0(t)\left(\mathbf{u}(\mathbf{z}_g, t) - \mathbf{u}_0(\mathbf{z}_g, t)\right) \\ &\quad - \dot{\boldsymbol{\chi}}(\mathbf{u}, t), \end{aligned} \tag{36}$$

where $\dot{\boldsymbol{\xi}}_d, \dot{\boldsymbol{\xi}}_0, \dot{\mathbf{y}}, \dot{\mathbf{y}}_d$ are essentially locally bounded, uniformly in t functions, $B_0(t)$ is the effectiveness matrix, an unknown, linear-parameterizable, essentially locally bounded function, $\dot{\boldsymbol{\chi}}$ is influence of the CF, which is essentially locally bounded function, $\mathbf{u}$ is the baseline control input. $\hat{B}_0 : \mathbb{R}^{4\times 14} \times [0, \infty) \to \mathbb{R}^{4\times 14}$ is the estimate of B_0. We assume that there exists an unknown parameter vector $\hat{\boldsymbol{\theta}} \in \mathbb{R}^k$ to be estimated such that j-column $\hat{\mathbf{b}}_j \in \mathbb{R}^k$ of $\hat{B}_0^T$ can be represented as

$$\hat{\mathbf{b}}_j = \Phi_j^T(\boldsymbol{\xi}_0, \mathbf{y}_0, \mathbf{u}_0, t)\hat{\boldsymbol{\theta}}, \tag{37}$$

where $\Phi_j^T(\boldsymbol{\xi}_0, \mathbf{y}_0, \mathbf{u}_0, t) : \mathbb{R}^{3\times 4\times 14} \times [0, \infty) \to \mathbb{R}^{4\times k}$ is the regressor function.

The estimation error is

$$\tilde{B}_0 = B_0 - \hat{B}_0. \tag{38}$$

In this case, the parameter estimation errors and its derivative are the following

$$\tilde{\boldsymbol{\theta}} = \boldsymbol{\theta} - \hat{\boldsymbol{\theta}}, \quad \dot{\tilde{\boldsymbol{\theta}}} = -\dot{\hat{\boldsymbol{\theta}}}. \tag{39}$$

For such a system, Lyapunov-based estimation algorithm can be designed

$$\dot{\hat{\boldsymbol{\theta}}} = -\nu\Gamma\Phi_j^T(\mathbf{x}_0, \mathbf{u}_0)\bar{\mathbf{z}}_y\Delta\mathbf{u}_j, \tag{40}$$

where $\Gamma \in \mathbb{R}^+$ are positive adaptation gains, $\Delta\mathbf{u}_j$ is jth element of $\Delta\mathbf{u}$, and

$$\nu = \begin{cases} 1, & \text{if } |T_{stat}| > T_{\alpha/2} \\ 0, & \text{if } |T_{stat}| < T_{\alpha/2} \end{cases}.$$

6.3. Proof of stability

Let $\boldsymbol{\zeta}\left(\mathbf{z}_\xi, \bar{\mathbf{z}}_y, \tilde{\boldsymbol{\theta}}\right) \in \mathbb{R}^{7+k}$ be defined as $\boldsymbol{\zeta} = \begin{bmatrix} \mathbf{z}_\xi^T & \bar{\mathbf{z}}_y^T & \tilde{\boldsymbol{\theta}}^T \end{bmatrix}^T$. The following regular CLF is selected to consider the stability of the system

$$V_{ad}(\boldsymbol{\zeta}) \triangleq \frac{1}{2}\mathbf{z}_\xi^T\mathbf{z}_\xi + \frac{1}{2a}\bar{\mathbf{z}}_y^T\bar{\mathbf{z}}_y + \frac{1}{2}\tilde{\boldsymbol{\theta}}^T\Gamma^{-1}\tilde{\boldsymbol{\theta}}. \tag{41}$$

The CLF in (41) complies with the following inequalities:

$$0 < W_1(\boldsymbol{\zeta}) \le V_{ad}(\boldsymbol{\zeta}, t) \le W_2(\boldsymbol{\zeta}), \text{ for } \boldsymbol{\zeta} \ne 0, \tag{42}$$

where the continuous positive-definite functions $W_1, W_2 : \mathbb{R}^{7+k} \to \mathbb{R}^+$ are defined as $W_1 \triangleq \lambda_1\|\boldsymbol{\zeta}\|^2$ and $W_2 \triangleq \lambda_2\|\boldsymbol{\zeta}\|^2$, where $\lambda_1, \lambda_2 \in \mathbb{R}^+$ are known constants. Then, $\dot{V}_{ad}(\boldsymbol{\zeta}(t), t) \overset{\text{a.e.}}{\in} \dot{V}(\boldsymbol{\zeta}(t), t)$ and

$$\dot{V} \triangleq \bigcap_{\eta\in\partial V_{ad}} \eta^T K \begin{bmatrix} \dot{\mathbf{z}}_\xi \\ \dot{\bar{\mathbf{z}}}_y \\ \dot{\tilde{\boldsymbol{\theta}}} \\ 1 \end{bmatrix} \left(\mathbf{z}_\xi, \bar{\mathbf{z}}_y, \tilde{\boldsymbol{\theta}}, t\right).$$

The CLF is C^∞ in $\boldsymbol{\zeta}$, then

$$\dot{\tilde{V}} \subset \nabla V_{ad}^T K \begin{bmatrix} \dot{\mathbf{z}}_\xi \\ \dot{\bar{\mathbf{z}}}_y \\ \dot{\tilde{\boldsymbol{\theta}}} \end{bmatrix} \left(\mathbf{z}_\xi \bar{\mathbf{z}}_y \tilde{\boldsymbol{\theta}}\right) \subset \left[\mathbf{z}_\xi^T, \bar{\mathbf{z}}_y^T, \tilde{\boldsymbol{\theta}}^T\Gamma^{-1}\right] K \begin{bmatrix} \dot{\mathbf{z}}_\xi \\ \dot{\bar{\mathbf{z}}}_y \\ \dot{\tilde{\boldsymbol{\theta}}} \end{bmatrix} \left(\mathbf{z}_\xi \bar{\mathbf{z}}_y \tilde{\boldsymbol{\theta}}\right). \tag{43}$$

The relationship (43) can be stated in the following form:

$$\begin{aligned} \dot{\tilde{V}}_{ad} &\subset \mathbf{z}_\xi\left(\dot{\boldsymbol{\xi}}_d - \dot{\boldsymbol{\xi}}_0 - T_\xi(\boldsymbol{\omega} - \boldsymbol{\omega}_0)\right) + \bar{\mathbf{z}}_y\left(\dot{\mathbf{y}}(\bar{\mathbf{z}}_y, t)\right. \\ &\quad \left. + B_0(t)\Delta\mathbf{u}(\bar{\mathbf{z}}_y, t) - \dot{\mathbf{y}}_d(t) - \dot{\boldsymbol{\chi}}(\bar{\mathbf{z}}_y, t)\right) + \\ &\quad + \tilde{\boldsymbol{\theta}}\left(-sign(\nu)\Gamma\Phi_j^T(\mathbf{x}_0, \mathbf{u}_0)\bar{\mathbf{z}}_y\Delta\mathbf{u}_j\right) = \\ &= -\mathbf{z}_\xi^T W_\xi \mathbf{z}_\xi - \frac{1}{a}\mathbf{z}_y^T W_y \mathbf{z}_y - \frac{1}{a}\mathbf{z}_y^T\tilde{B}_0\Delta\mathbf{u} - \tilde{\boldsymbol{\theta}}^T\nu\Gamma^{-1}\dot{\hat{\boldsymbol{\theta}}} \\ &= -\mathbf{z}_\xi^T W_\xi \mathbf{z}_\xi - \frac{1}{a}\mathbf{z}_y^T W_y \mathbf{z}_y. \end{aligned} \tag{44}$$

Since W_ξ and W_y are the positive symmetric matrices, then

$$\dot{\tilde{V}}_{ad}(\zeta, t) \le W_3(\zeta) = -\rho\|\zeta\|^2. \tag{45}$$

Since the $W_3(\zeta)$ does not depend on ν, it follows that (45) is true almost everywhere. Thus, according to Theorem 2 this proves that the equilibrium $\begin{bmatrix} \mathbf{z}_\xi^T & \bar{\mathbf{z}}_y^T & \tilde{\boldsymbol{\theta}}^T \end{bmatrix} = 0$ is uniformly asymptotically stable.

6.4. Recursive least squares

Described above second-layer estimator based on the TF approach is compared here with the EF RLS estimator.

Similar to the combined effectiveness, the identification problem is stated as follows:

$$\boldsymbol{\varsigma} \cong \mathbf{A}\hat{\boldsymbol{\theta}}, \tag{46}$$

where the response variable vector is the following

$$\begin{aligned} \boldsymbol{\varsigma} = [&\Delta\dot{y}_m^{ind}(1) - W_s D_u \hat{B}_0 \Delta\mathbf{u}^{\sup}(1) \\ &\Delta\dot{y}_m^{ind}(2) - W_s D_u \hat{B}_0 \Delta\mathbf{u}^{\sup}(2) \ldots \\ &\Delta\dot{y}_m^{ind}(N) - W_s D_u \hat{B}_0 \Delta\mathbf{u}^{\sup}(N)], \end{aligned}$$

$\Delta\dot{y}_m^{ind}(1)\,\Delta\dot{y}_m^{ind}(2)\ldots\Delta\dot{y}_m^{ind}(N)$ is the record of derivative increment for m component of the dynamic state vector $\mathbf{y}$, the predictor variable vector is based on the incremental signal for the control surface under study

$$\mathbf{A} = \left[\Delta\mathrm{u}^{ind}(1)\,\Delta\mathrm{u}^{ind}(2)\ldots\Delta\mathrm{u}^{ind}(N)\right]^T,$$

D_u is the allocation matrix, W_s is the amplification matrix required to produce the supporting control signal $\mathbf{u}^{\sup}$. Elements of W_s specify how the individual actuator signals differ from the generic one. The terms $-W_s D_u \hat{B}_0 \mathbf{u}^{\sup}(i)$, $i = 1\ldots N$, which are responsible for the subtraction of contribution from the supporting signal to the flight dynamics, are introduced in order to obtain the pure dynamics produced by the treated control surface. We used the modified EF RLS [35] to solve (46).

7. Simulation results

In this section, a simulation study of the ability of the discussed algorithms to tackle the failures is considered.

A nonlinear model of the Boeing 747 aircraft, courteously provided by the consortium partner TU Munich, is used to validate the designed approach. This model is a variant of the GARTEUR RECOVER benchmark simulator [7]. The Boeing 747 is a large, transport aircraft with four wing-mounted engines. It has a length of

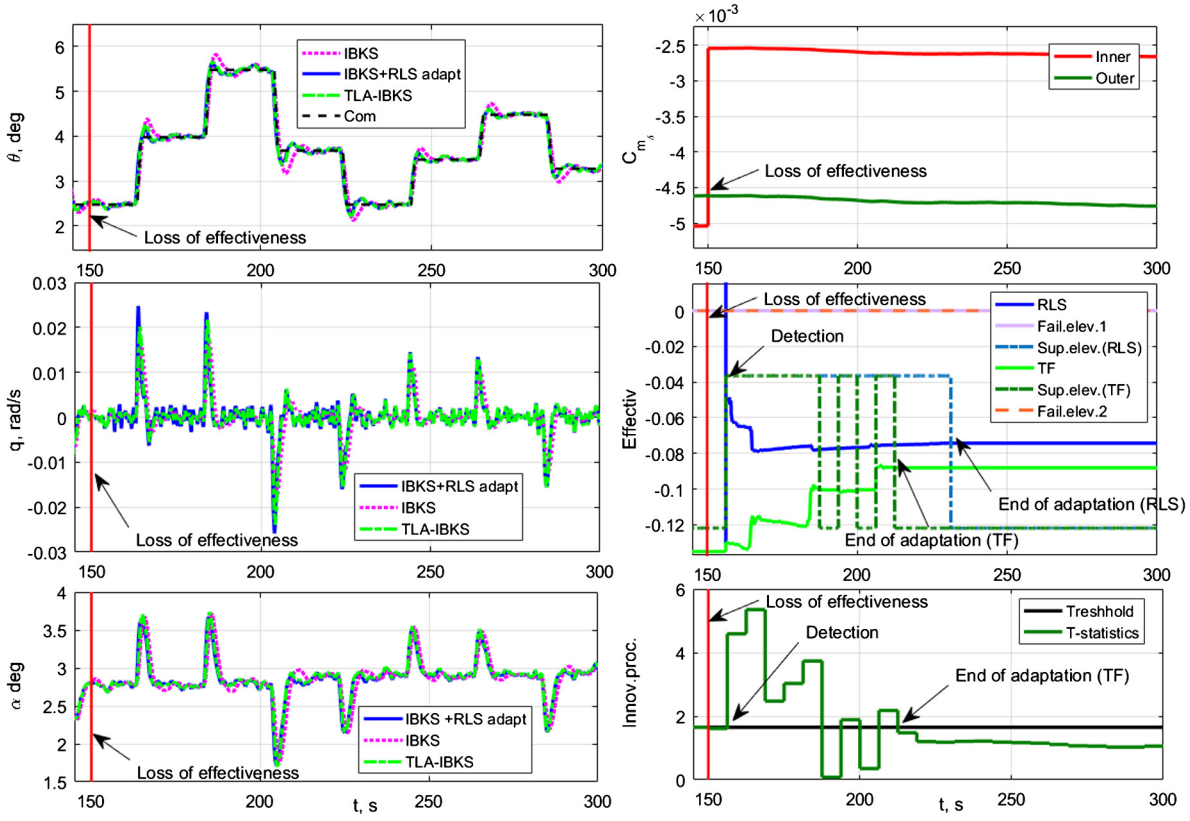

Fig. 4. Two failures and loss of effectiveness. (For interpretation of the colours in the figure(s), the reader is referred to the web version of this article.)

approximately 70 meters, wingspan of 60 meters, and the maximum take-off weight is greater than 300 tons. The actuation of the Boeing 747 simulator corresponds to four ailerons, four elevators, two rudders, and four engines.

The nominal condition from which the simulation starts is a straight flight towards North with 340 knots of True Airspeed (TAS) and at an altitude of 5000 ft. The flight is developed under a low turbulence condition defined by a 20-feet wind of 15 m/s in North direction and a turbulence intensity exceedance probability of 0.01. In the current research, a longitudinal motion is considered.

Parameters of the first layer: Forgetting function of the modified EF RLS for the first layer $F = 0.99999I + 0.000002P(t-1)$ is the same for all algorithms of the second layer. Tolerance to the noise in (26) is $b = 0.03$ for modified EF RLS and $b = 0.01$ for TFs. A significance level for the T-statistics is $\alpha = 5$.

Parameters of the second layer: Adaptation gain for the TF update law is $\Gamma = 300$. Forgetting function of EF RLS, which is used for comparison purposes at the second layer, is $F = 0.99995I + 0.000007P(t-1)$.

The performance of the proposed scheme is validated for the cases of multiple failures. The detailed explanation of the scenarios is given below.

7.1. Two failures and loss of effectiveness

In the current section an ability of the developed controller is evaluated in a case of a two failures (stuck-in-position) and a partial loss of effectiveness of the third elevator. Due to this failure, the effectiveness of the elevator is reduced by 50 percent.

The results are presented in Fig. 4. Here it is assumed that two elevators failed before $t = 0$ s. For the adaptive algorithm, it is considered that these two failures detected and isolated also before $t = 0$ s, which means that corresponding coefficients equal to zero in the $\hat{B}_0$. The loss of effectiveness of one the two rest elevators simulated at $t = 150$ s.

On the left subplots the pitch angle, pitch rate and angle of attack θ, q, α are presented. On the right-top subplot the real effectiveness of two working elevators, namely, inner and outer elevators, are demonstrated. One can see that at $t = 150$ s the effectiveness of the inner elevator degraded. On the middle-right subplot the coefficients in the effectiveness matrix $\hat{B}_0$ are demonstrated. Green solid line corresponds to estimation of the effectiveness of the third elevator with partial loss of effectiveness at $t = 150$ s obtained by the proposed algorithm. The estimation obtained using RLS algorithm is coplotted with the solid green line for comparison purpose. Effectiveness of the elevators failed before $t = 0$ s is zero. Dash-dotted green (TF) and blue lines (RLS) are effectiveness of the "supporting" elevator, which usage is artificially reduced during identification according to W_s during the identification manoeuvres. On the bottom-right subplot an evolution of the innovation process for the proposed TF approach demonstrates governing process of the adaptation; the innovation process for the RLS is not plotted to avoid overload of the figure. From the pitch angle θ subplot (top-left) one can conclude that the tracking performance of the adaptive strategies is improved as compared to the baseline controller.

T-criterion is used to govern the identification process. The threshold for the T-criterion is violated after failure, the system detects the failure and starts identification. As soon as the algorithm gets a new value of the effectiveness, the T-criterion goes below the threshold and stops estimations. From the presented results, it can be concluded that it is an iterative process and T-statistics goes below and above the threshold value several times before the final convergence. Eventually, when the process converges, the T-criterion stays beyond the threshold value, the estimation of failed elevator effectiveness is completed and the value of the reduced "supporting" elevator recovers back to its initial value. It should

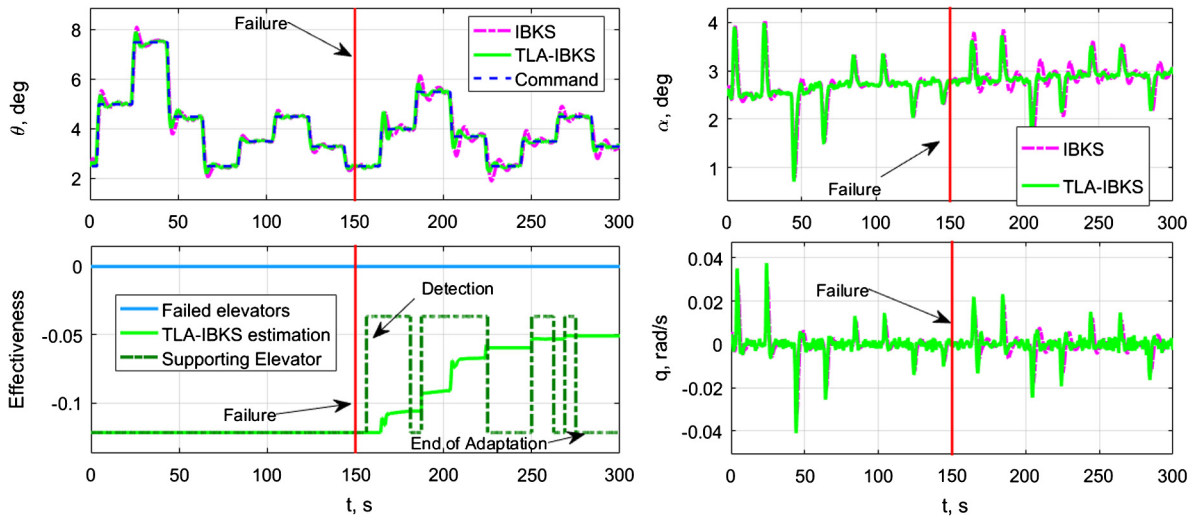

Fig. 5. Comparison of IBKS and TLA-IBKS algorithm: 1st order nonlinear dynamics.

be mentioned that when T-statistics is below the significance level before the final convergence of the algorithm, the adaptation process is stopped and, thus, a slower convergence rate of the estimation algorithm is implemented. However, it helps to reduce the excessive excitation of the system.

7.2. First order dynamics

Results obtained in the previous section for a partial loss of effectiveness correlates with the results of the other researchers [33], [43] manifesting robustness of the IBKS to actuator failures conserving the system input affine property. In the current section, we would like to go ahead and investigate the property of the IBKS and proposed TLA-IBKS controllers under failures breaking this property. For example, this section considers the presence of the first order unmodelled actuator dynamics.

High level of redundancy (four elevators) allows conserving the input affine property for Boeing 747 even for the case of appearance of unmodelled dynamics in one of the actuators. To simulate the conditions where the input affine property is not valid anymore we assume here that two elevators failed (before $t = 0$ s) and in one of the rest operating elevators an unmodelled dynamics has arisen. For the adaptive algorithm, it is again considered that these two elevator failures were detected and isolated before $t = 0$ s and those corresponding coefficients equal to zero in $\hat{B}_0$. Meanwhile, for the pure IBKS, it is considered, that the algorithm does not have access to new information about the control effectiveness, and thus, uses initial matrix $\hat{B}_0$. At $t = 150$ s, the nonlinear unmodelled dynamics arises at one of the two working actuators as a result of a failure. It was reported that many known actuator failures can be simulated with the first or second order actuator dynamics [36], [37]. For the current scenario, we assumed the first order dynamics, represented with the following equation

$$F(s) = (2s + 1)^{-1}. \tag{47}$$

Comparison of behaviours of the baseline IBKS controller and the TLA-IBKS is presented in Fig. 5.

The figure shows the parameters of the state vector θ, q, α along with estimates of the effectiveness of the elevator for TLA-IBKS. Before $t = 150$ s, the IBKS demonstrates robustness to failures, namely, even with two failed elevators it follows the reference signal. At the same time, the tracking error of the TLA-IBKS is reduced as compared to the baseline IBKS because of updated knowledge of $\hat{B}_0$. The first order actuator dynamics arose at $t = 150$ s has a significant effect on the performance of the IBKS algorithm, namely, weakly damped oscillations are observed in the state vector parameters θ, q, α. Augmentation of the baseline controller with adaptive element cancels this undesired behaviour of the system. Operation of the TL-adaptation algorithm is demonstrated in the bottom-left subplot. The effectivenesses of all elevators are illustrated, two elevators are failed before $t = 0$ s, one is operating and producing the supporting signal, and effectiveness of the fourth one is estimated. For the supporting signal, one can see switching from nominal $\hat{B}_0$ values ≈ -0.12 to reduced $\hat{B}_0$ values ≈ -0.036 and back. These switches are produced when T-statistics of the first layer algorithm goes above and below the significance level. The estimation algorithm iteratively convergences similar to the previous case, and the first layer estimator governs the system identification rate.

Proposed TF estimator is compared with RLS estimator and results are presented in Fig. 6.

In the figure, plots of transition processes of state vector parameters θ, q, α together with elevator effectiveness estimations are given. On the effectiveness subplot (bottom-left subplot), two supporting signals and two estimations, corresponding to TF and RLS algorithms, are shown here. Convergence of the RLS algorithm is slightly faster than TF. The RLS performs abrupt adaptation during the first seconds. The TF approach produces adaptation slightly slower, however, along the trajectories, guaranteeing the system stability (40). The performances of both algorithms starting from $t \approx 230$ s are almost undistinguishable. However, pithing rate oscillation level is higher for RLS adaptation strategy (has higher peaks), and thus could have more harm effect on the performance, for example, on the passenger comfort.

7.3. Second order dynamics

As it is shown in the previous section, presence of uncertainty in the form of non-linear dynamics in actuators could cause a degradation of the system performance since the input affine property is not valid anymore. In this section, this issue is further studied. Particularly, presence of non-linear dynamics of the second order in one of the actuators is presented. Similar to the previous test cases, we assume that two elevators failed before $t = 0$ s, for the adaptive controller, it is considered that these two failures detected and isolated before $t = 0$ s and those corresponding coefficients equal to zero in $\hat{B}_0$. At $t = 150$ s the nonlinear unmodelled

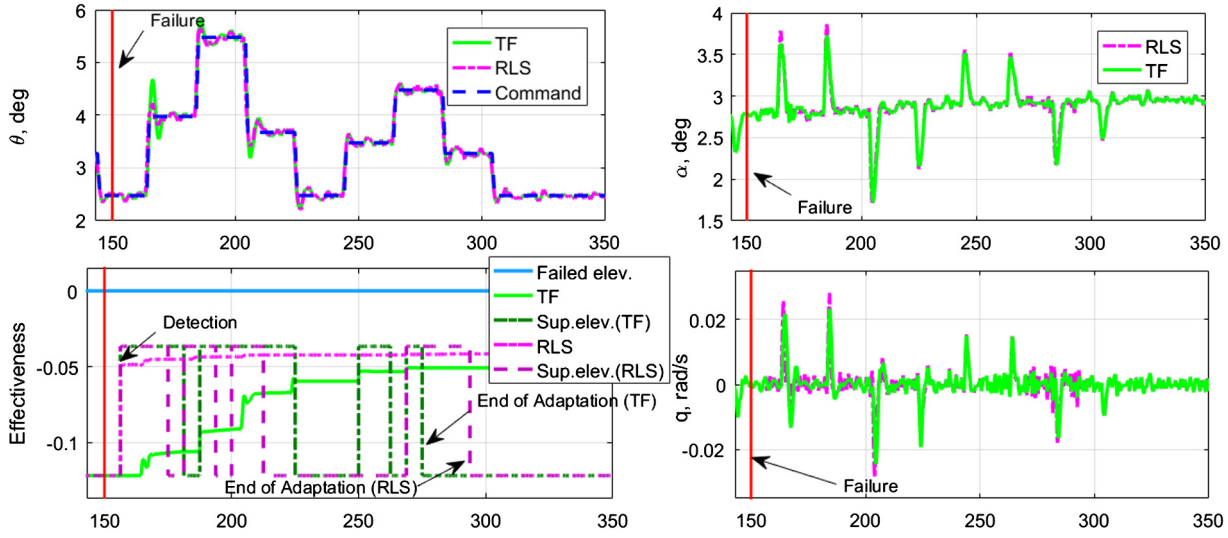

Fig. 6. Comparison of EF RLS and TF adaptive algorithm: 1st order nonlinear dynamics.

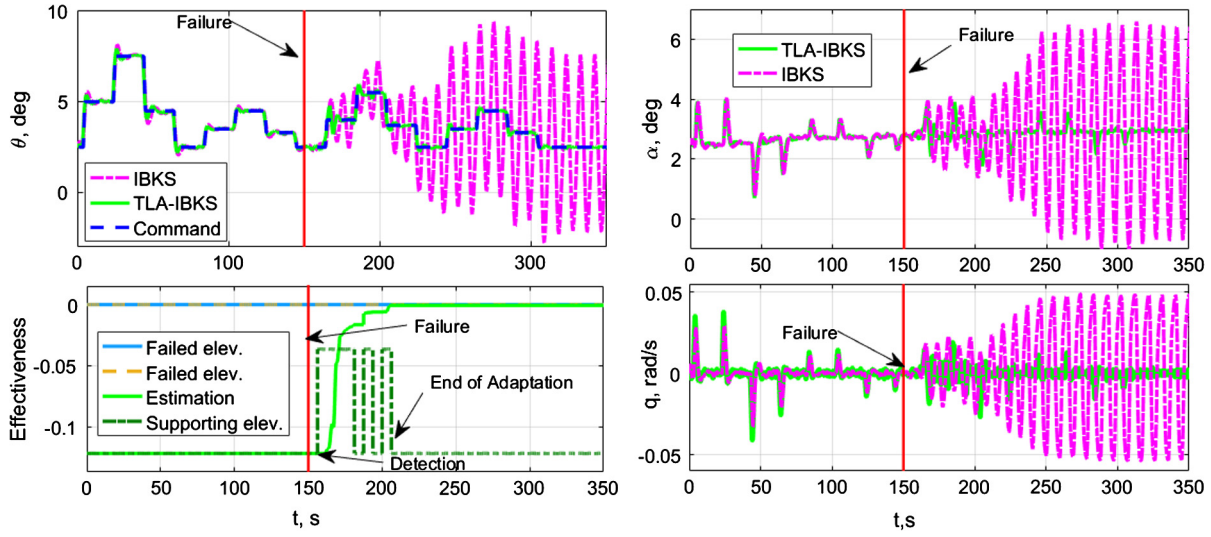

Fig. 7. Comparison of IBKS and TLA-IBKS: 2nd order nonlinear dynamics.

dynamics arises at the one of the two working actuators as a result of failure, which can be modelled by the second order dynamics:

$$F(s) = \left(2s^2 + s + 1\right)^{-1}. \tag{48}$$

Shown in Fig. 7 is comparison between behaviour of IBKS and Adaptive IBKS in considered case.

Similar to the previous figures, the transition processes of state vector parameters θ, q, α are provided in the top-left, top-right and bottom-right subplots correspondingly. Convergence of the effectiveness estimations is demonstrated in the bottom-left subplot of the figure. From the figure, one can see that under the presence of 2-nd order dynamics the IBKS control suffers from the instability in the form of high-amplitude limit-cycle oscillations. Such a nonlinear dynamics is caused by interaction between failed and non-failed elevators. Meantime, TLA-IBKS manifests the system stability and good tracking performance.

The proposed TF estimator is compared with the RLS-based estimator in Fig. 8. Both algorithms provide stability. RLS has larger estimation rate at the initial stage and thus provides faster adaptation and less oscillatory behaviour because it "switch off" the failed elevator faster than TF.

8. Conclusions

Incremental Backstepping is recently developed technique with a reduced dependency on the on-board aircraft model. This approach uses estimates of the state derivatives and the current actuator states to linearize the flight dynamics with respect to current state. Our results and also results of the other researchers revealed robustness of the IBKS to actuator failures when the system remains input affine, even for the case of multiple failures. However, as we have shown in the current study, in severe conditions, with a combination of multiple failures and presence of unmodelled actuator dynamics, the system dynamics might loss its input affine property. Such conditions might be a case for not only scenarios considered in the current study but also for some others, for example, in case of partial loss of effectiveness and large transport delay. As a result, the stability of the system cannot be guaranteed anymore and adaptive augmentation is required to compensate the unmodelled dynamics.

In this research, Two-Layer Adaptive augmentation for Incremental Backstepping Flight Control, which was capable to tackle possible actuator failures, was proposed. At the first layer, the system performs monitoring of the combined control effectiveness, compares estimated values with the values obtained previously

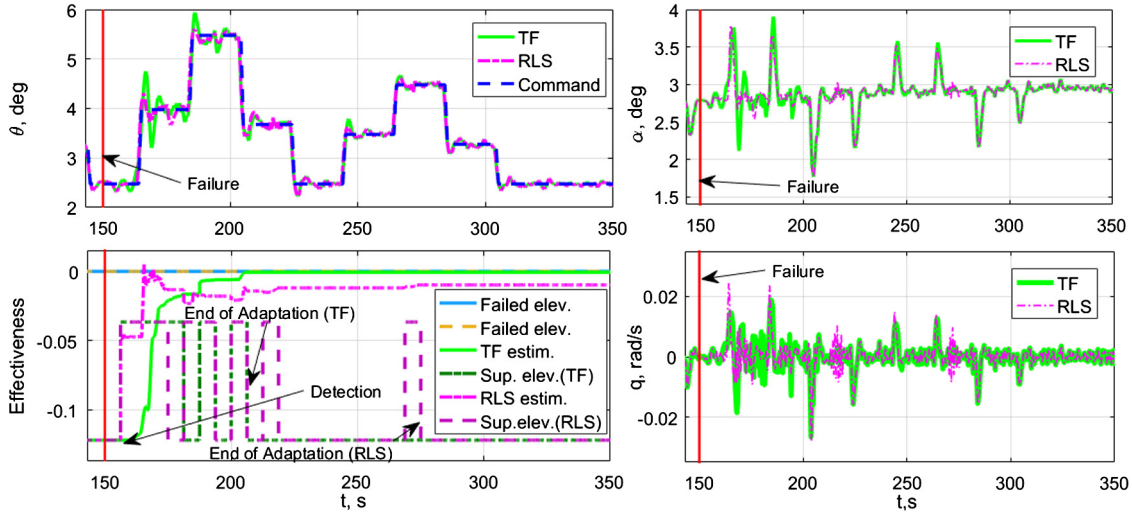

Fig. 8. Comparison of RLS and TF estimators: 2nd order nonlinear dynamics.

and calculates T-statistics. If T-statistics violates the significance level, the system detects possible anomalies through it. In case of an anomaly detection, the algorithm initiates the second-layer estimation determining the individual effectiveness and provides updated information about the effectiveness matrix to the baseline controller. Such two-layer structure requires less excitation of the system, thus, increases comfort and tracking performance. In addition, fault isolation in the form of control effectiveness identification increases tolerance to faults since does not require information on a failure type and can be used for unforeseen failures.

From the theoretical point of view, the closed-loop dynamics of the system augmented with TLA becomes nonsmooth. Filippov generalization for nonlinear differential equations with discontinuous right-hand sides was applied to develop Lyapunov based TF adaptive law for the second layer adaptation. Uniform asymptotic stability for the proposed estimation procedure was proven.

Performance of the TLA-IBKS was studied in simulations of three different failure scenarios developed for Boeing 747 involving multiple failures, partial loss of effectiveness, unmodelled actuator dynamics of the first and the second orders. Our results manifested improved stability and tracking performance characteristics of the TLA-IBKS controller as compared to the baseline IBKS. In particular, information that is more precise provided to the baseline controller by the developed TLA augmentation improved tracking performance for the case of loss of effectiveness, cancelled undesired oscillations observed for the IBKS in case of first order actuator dynamics and prevented from a loss of stability for the second-order actuator dynamics. TF second layer estimator performance is evaluated by comparison with RLS estimator. Performance of both estimators are very similar, however, the proposed TF approach is preferred since the stability of the system can be guaranteed from the theoretical point of view.

Declaration of competing interest

The authors declare that they have no known competing financial interests or personal relationships that could have appeared to influence the work reported in this paper.

Acknowledgements

This research is funded by the European Union in the scope of INCEPTION project, which has received funding from the EU's Horizon2020 Research and Innovation Programme under grant agreement No. 723515.

References

[1] EASA, European Aviation Safety Agency. Annual Safety Review 2014, 2014.
[2] N.B. Abramov, M.G. Goman, A.N. Khrabrov, B.I. Soemarwoto, Aerodynamic modeling for poststall flight simulation of a transport airplane, J. Aircr. 56 (4) (2019) 1427–1440, https://doi.org/10.2514/1.c034790.
[3] A.M. Murch, J.V. Foster, Recent NASA research on aerodynamic modeling of post-stall and spin dynamics of large transport airplanes, in: Collect. Tech. Pap. - 45th AIAA Aerosp. Sci. Meet., 8 January, 2007, pp. 5553–5572.
[4] D.I. Ignatyev, M.E. Sidoryuk, K.A. Kolinko, A.N. Khrabrov, Dynamic rig for validation of control algorithms at high angles of attack, J. Aircr. 54 (5) (2017) 1760–1771, https://doi.org/10.2514/1.C034167.
[5] D. Ignatyev, A. Khrabrov, Experimental study and neural network modeling of aerodynamic characteristics of canard aircraft at high angles of attack, Aerospace 5 (1) (2018), https://doi.org/10.3390/aerospace5010026.
[6] M.G. Goman, A.V. Khramtsovsky, E.N. Kolesnikov, Evaluation of aircraft performance and maneuverability by computation of attainable equilibrium sets, J. Guid. Control Dyn. 31 (2) (2008) 329–339, https://doi.org/10.2514/1.29336.
[7] H. Smaili, B. Jan, T. Lombaerts, O. Stroosma, A benchmark for fault tolerant flight control evaluation, IFAC Proc. Vol. (December 2009) 241–246, https://doi.org/10.3182/20090630-4-ES-2003.0246.
[8] D.I. Ignatyev, A.N. Khrabrov, Neural network modeling of unsteady aerodynamic characteristics at high angles of attack, Aerosp. Sci. Technol. 41 (2015) 106–115, https://doi.org/10.1016/j.ast.2014.12.017.
[9] T. Yucelen, A.J. Calise, Derivative-free model reference adaptive control, J. Guid. Control Dyn. 34 (4) (2012) 933–950, https://doi.org/10.2514/1.53234.
[10] N. Hovakimyan, C. Cao, L1 adaptive control theory: guaranteed robustness with fast adaptation 34 (4) (2010).
[11] G.P. Falconi, C.D. Heise, F. Holzapfel, Novel stability analysis of direct MRAC with redundant inputs, in: 24th Mediterr. Conf. Control Autom. MED 2016, 2016, pp. 176–181.
[12] Q.P. Chu, D.A. Joosten, M.H. Smaili, O. Stroosma, T.J.J. Lombaerts, J.A. Mulder, Piloted simulator evaluation results of new fault-tolerant flight control algorithm, J. Guid. Control Dyn. 32 (6) (2009) 1747–1765, https://doi.org/10.2514/1.44280.
[13] J.H. Blakelock, Automatic Control of Aircraft and Missiles, 2nd ed., Wiley, New York, 1991.
[14] S.P. Shue, M.E. Sawan, K. Rokhsaz, Mixed H/H8 method suitable for gain scheduled aircraft control, J. Guid. Control Dyn. 20 (4) (1997) 699–706.
[15] J.-J.E. Slotine, W. Li, Applied nonlinear control 62 (7) (1991).
[16] Antonios Tsourdos, Brian White, Adaptive flight control design for nonlinear missile, Control Eng. Pract. 13 (3) (2005) 373–382.
[17] M. Krstic, P.V. Kokotovic, I. Kanellakopoulos, Nonlinear and Adaptive Control Design, 1st ed., John Wiley & Sons, Inc., USA, 1995.
[18] C.-H. Lee, T.-H. Kim, M.-J. Tahk, Agile missile autopilot design using nonlinear backstepping control with time-delay adaptation, Trans. Jpn. Soc. Aeronaut. Space Sci. 57 (1) (2014) 9–20, https://doi.org/10.2322/tjsass.57.9.
[19] J.R. Azinheira, A. Moutinho, E.C. De Paiva, Airship hover stabilization using a backstepping control approach, J. Guid. Control Dyn. 29 (4) (Jul. 2006) 903–914, https://doi.org/10.2514/1.17334.
[20] L.G. Sun, C.C. de Visser, Q.P. Chu, W. Falkena, Hybrid sensor-based backstepping control approach with its application to fault-tolerant flight control, J. Guid. Control Dyn. 37 (1) (2013) 59–71, https://doi.org/10.2514/1.61890.
[21] J. Hu, J. Huang, Z. Gao, H. Gu, Position tracking control of a helicopter in ground effect using nonlinear disturbance observer-based incremental back-

stepping approach, Aerosp. Sci. Technol. 81 (Oct. 2018) 167–178, https://doi.org/10.1016/J.AST.2018.08.002.
[22] S. Sieberling, Q.P. Chu, J.A. Mulder, Robust flight control using incremental nonlinear dynamic inversion and angular acceleration prediction, J. Guid. Control Dyn. 33 (6) (Nov. 2010) 1732–1742, https://doi.org/10.2514/1.49978.
[23] P. van Gils, E.-J. Van Kampen, C.C. de Visser, Q.P. Chu, Adaptive incremental backstepping flight control for a high-performance aircraft with uncertainties, in: AIAA Guid. Navig. Control Conf., January, 2016.
[24] P. Bhardwaj, V.S. Akkinapalli, J. Zhang, S. Saboo, F. Holzapfel, Adaptive augmentation of incremental nonlinear dynamic inversion controller for an extended f-16 model, in: AIAA Scitech 2019 Forum, January, 2019, pp. 1–21.
[25] J. Chang, Z. Guo, J. Cieslak, W. Chen, Integrated guidance and control design for the hypersonic interceptor based on adaptive incremental backstepping technique, Aerosp. Sci. Technol. 89 (Jun. 2019) 318–332, https://doi.org/10.1016/J.AST.2019.03.058.
[26] G.P. Falconi, V.A. Marvakov, F. Holzapfel, Fault tolerant control for a hexarotor system using incremental backstepping, in: 2016 IEEE Conf. Control Appl. CCA 2016, 2016, pp. 237–242, no. 1.
[27] V.S. Akkinapalli, G.P. Falconi, F. Holzapfel, Fault tolerant incremental attitude control using online parameter estimation for a multicopter system, in: 2017 25th Mediterr. Conf. Control Autom. MED 2017, 2017, pp. 454–460.
[28] D.I. Ignatyev, H.S. Shin, A. Tsourdos, Two-layer on-line parameter estimation for adaptive incremental backstepping flight control for a transport aircraft in uncertain conditions, IFAC-PapersOnLine 52 (12) (2019) 411–416, https://doi.org/10.1016/j.ifacol.2019.11.278.
[29] V. Klein, E. Morelli, Aircraft System Identification - Theory and Practice, AIAA, Inc., Blacksburg, USA, 2006.
[30] Karl Johan Åstrom, Björn Wittenmark, Adaptive Control, 2nd ed., Addison-Wesley Longman Publishing Co., Inc., Boston, MA, USA, 1994.
[31] https://inception-h2020.tekever.com/.
[32] R.A. Cordeiro, R. Azinheira, A. Moutinho, Cascaded incremental backstepping controller for the attitude tracking of fixed-wing aircraft, in: 5th CEAS Conference on Guidance, Navigation and Control, 2019.
[33] R.A. Cordeiro, J.R. Azinheira, A. Moutinho, Addressing actuation redundancies in incremental controllers for attitude tracking of fixed-wing aircraft, IFAC-PapersOnLine 52 (12) (2019) 417–422, https://doi.org/10.1016/j.ifacol.2019.11.279.
[34] D.I. Ignatyev, H.S. Shin, A. Tsourdos, Two-layer fault detection for incremental flight control of fixed-wing UAV, in: 2019 Int. Work. Res. Educ. Dev. Unmanned Aer. Syst. RED-UAS 2019, 2019, pp. 227–236, https://doi.org/10.1109/REDUAS47371.2019.8999692.
[35] H.-S. Shin, H.-I. Lee, A New Exponential Forgetting Algorithm for Recursive Least-Squares Parameter Estimation. Available at: http://arxiv.org/abs/2004.03910, April 2020.
[36] J.D. Bošković, R.K. Mehra, Failure detection, identification and reconfiguration system for a redundant actuator assembly, IFAC Proc. Vol. 36 (5) (2003) 411–416, https://doi.org/10.1016/S1474-6670(17)36526-6.
[37] J.D. Bošković, S.E. Bergstrom, R.K. Mehra, Adaptive accommodation of failures in second-order flight control actuators with measurable rates, Proc. Am. Control Conf. 2 (July 2005) 1033–1038, https://doi.org/10.1109/acc.2005.1470096.
[38] T.W. Anderson, An Introduction to Multivariate Statistical Analysis, 3rd edition, 2003, New Jersey, USA.
[39] A.F. Filippov, Differential Equations with Discontinuous Righthand Sides, Springer, Netherlands, 1988.
[40] F.H. Clarke, Optimization and Nonsmooth Analysis, Society for Industrial and Applied Mathematics, 1983.
[41] D. Shevitz, B. Paden, Lyapunov stability theory of nonsmooth systems, IEEE Trans. Autom. Control 39 (9) (1994) 1910–1914, https://doi.org/10.1109/9.317122.
[42] H.K. Khalil, Nonlinear Systems, 2nd ed., Prentice Hall, Upper Saddle River, USA, 1996.
[43] B.-J. Jeon, M.-G. Seo, H.-S. Shin, A. Tsourdos, Understandings of classical and incremental backstepping controllers with model uncertainties, IEEE Trans. Aerosp. Electron. Syst. (2019) 1, https://doi.org/10.1109/taes.2019.2952631.

2020-07-01

Two-layer adaptive augmentation for incremental backstepping flight control of transport aircraft in uncertain conditions

Ignatyev, Dmitry I.

Elsevier

Ignatyev DI, Shin H-S, Tsourdos A. (2020) Two-layer adaptive augmentation for incremental backstepping flight control of transport aircraft in uncertain conditions. Aerospace Science and Technology, Volume 105, October 2020, Article number 106051

https://doi.org/10.1016/j.ast.2020.106051